

Research Paper

GIS and SWAT Model-Based Assessment of Theoretical Hydropower Potential in the Furfuro Watershed, Ethiopia

Amsayaw Genet^{1*}, Aynadis Ejargew², Temesgen Zelalem¹, Abebe Tadesse³, Tensay Kifle⁴, Moges Tariku¹

¹Department of Hydraulic Engineering, Wolkite University, Wolkite, Ethiopia

²Department of Water Resource and Irrigation Engineering, Dilla University, Dilla, Ethiopia

³Department of Hydraulic Engineering, Hawassa University, Hawassa, Ethiopia

⁴Department of Water Supply and Environmental Engineering, Werabe University, Werabe, Ethiopia

Abstract

Article History:

Received: 04 March 2025

Accepted: 23 December 2024

Published online: 06

January 2026

Keywords:

Analytic Hierarchy

Process, Furfuro

Watershed, GIS,

Theoretical

Hydropower,

Renewable Energy,

Run-of-River

Hydropower Plant,

SWAT

Ethiopia possesses abundant water resources and favourable topography for hydropower development. However, there is a scarcity of comprehensive data on many perennial rivers and their hydropower potential. For Ethiopia to realize its enormous hydropower potential and move closer to a sustainable and clean energy future, accurate information is essential. This study used Geographic Information Systems (GIS) and the Soil and Water Assessment Tool (SWAT) to assess the Furfuro River's potential for hydropower in Ethiopia's Rift Valley Basin. The SWAT model was established for the Furfuro watershed, incorporating DEM, soil, land use, meteorological, and river flow data. Using SWAT, the Furfuro watershed was split up into 31 subbasins and 265 Hydraulic Response Units (HRUs). We calibrated and validated the model using the Sequential Uncertainty Fitting Version 2 (SUFI-2). During calibration, model performance was evaluated using NSE, R^2 , and PBIAS. The values were 0.68, 0.69, and -0.8%, respectively. During validation, the values were 0.67, 0.7, and 2.9%, respectively. The study identified four potential hydropower sites in the Furfuro River, all located on 4th and 5th-order streams with heads of 3 meters or more. These sites were ranked based on a suitability index using an analytical hierarchy process. With a theoretical hydropower potential of 0.297 MW and 0.36 m³/s discharge at 95% exceedance, Site 1 is the most ideal, according to the analysis, while Site 4 is the least suitable, with a theoretical hydropower potential of 0.018 MW and 0.1 m³/s discharge at 95% exceedance. Therefore, the development of these small-scale hydropower potentials on the Furfuro River has the potential to offer the local population a clean and reasonably priced energy supply. The study illustrated the effectiveness of integrating GIS, SWAT modeling, and multicriteria decision analysis for hydropower site selection in data scarce regions.

Author email: amsayawgenet@gmail.com

DOI: <https://doi.org/10.70984/kjaqm893>

1. Introduction

Energy serves as an integral part of modern civilization and a key indicator of socioeconomic growth (Surendra et al., 2014). Numerous studies reported a direct relationship between a nation's economic growth and its energy usage (Mose & Kipchirchir, 2024; Sharmin & Khan, 2016). The importance of energy is especially significant for developing countries like Ethiopia, where on-demand electricity is essential for progressive economic reforms and job creation (Ebhotu & Tabakov, 2019). However, the shortage of traditional energy supplies in many developing nations and their dependence on imported fuels are causing an energy crisis. Ethiopia's energy economy, like many other sub-Saharan African countries, relies heavily on biomass and imported fuels.

In Sub-Saharan Africa, for instance, about 85% of people without power lived in rural areas (World Bank, 2011). In Ethiopia's rural areas, the scarcity of energy supply has become a persistent issue. Approximately 85% of Ethiopians reside in rural areas with less than 1% access to electricity. Access to electricity in rural areas has various constraints, mainly caused by a shortage of power, and their settlements are either too sparsely populated or too remote from the national grid, which could incur high transmission costs. Rural people often use kerosene, firewood, cow dung, and other conventional biomass resources to meet their energy needs. The cost of kerosene is rising due to higher fuel prices. These practices contribute to deforestation, soil erosion, and other environmental problems (Eshetu, 2024).

Additionally, traditional energy sourcing to meet these growing energy demands, development of sustainable renewable energy-generating systems in the rural areas are essential. The development and generation of sustainable power need a comprehensive study and

assessment of available resources. Having a reliable evaluation of the abundance and distribution of resources in a country aids future energy planning and the identification of promising locations for hydropower projects. This planning calls for an accurate evaluation of the available water resources, which is dependent on regional natural processes and topographic features (Bhattarai et al., 2024).

Traditional methods for assessing hydropower potential rely on historical discharge data from gauged locations. However, the complexity of hydrological processes and the scarcity of gauging stations make these techniques limited. These limitations can lead to inaccurate and unreliable assessments of hydropower potential, particularly for ungauged locations. Additionally, relying on location-specific data can exclude potential sites in other areas. The introduction of modern computational tools like Hydrological models, GIS, and Remote Sensing (RS) has effectively addressed the limitations of traditional hydropower potential assessment methods. These tools enable a comprehensive representation of terrain, complex hydrological phenomena, and varying climates, leading to more accurate and reliable assessments with the requirement of less physical data.

Head drop (H) and river discharge (Q) are two crucial variables that must be determined to evaluate hydropower potential. Topographic maps or Digital Elevation Models (DEM) can be used to compute the potential head drop, which is the elevation difference between a river's upstream and downstream sites (Ejargew et al., 2025), whereas the river flow data requires continuous readings from gauging sites.

To evaluate the hydropower potential in the perennial rivers, several researchers used a hydrological model (SWAT) combined with GIS and RS techniques. Kusre et al. (2010) investigated the hydropower potential of the

Kopili River watershed in Assam, India, using GIS and the SWAT model. The study employed the SWAT to assess the river's stream flow and GIS and RS to determine an appropriate hydropower potential head. To guarantee adequate potential head, a bottom gradient of greater than 2% was taken into account when conducting the potential head assessment.

Pandey et al. (2015) used SWAT modeling and geographical analysis to investigate the Mat River's hydropower potential in Mizoram, India. Only four years of streamflow data were used to train the SWAT simulation model. The flow simulation was analyzed considering streams larger than second order to guarantee adequate flow. However, training the model with short-period data records could give a biased estimation of flow. In addition, the average gradient along the stream's bottom was not considered in the analysis of the study.

A study by Moshe and Tegegne (2024) evaluated the run-of-river hydropower potential in Ethiopia's Omo-Gibe Basin, an area with limited data. The study used GIS-based multicriteria decision analysis to rank the potential sites, and the space between the hydropower schemes was permitted to range from 500 meters to three kilometers. Furthermore, the potential head was directly measured from the GIS digital feature class, which could bring a higher variation in the actual observed head. Another study by Anore et al. (2025) employed geospatial methodologies and GIS Multi-criteria decision-making to find possible hydropower generation sites in Ethiopia's Megecha watershed, Omo Gebie Basin. Anore et al. (2025) selected possible hydropower sites in the Megecha watershed using multi-criteria decision-making and the SWAT streamflow simulation. Another study on the Gumara River, Abbay Basin, by Mehari (2020) used SWAT simulation and the Multi-criteria decision-making, allowing the gap between two consecutive sites to be 500 m. Areri

& Bibi (2023) used GIS and the Hydrologic Engineering Center-Hydrologic Modeling System (HEC-HMS) hydrologic modeling technique to identify small-scale hydropower potential sites in the Awata River, Genale Dawa Basin, Ethiopia. In this study, streamflow was simulated using HEC-HMS, and the hydraulic head was calculated using DEM and the stream network. To identify suitable potential sites, the study identifies the suitable potential sites considering demand centers for power, stream flow, and the site's road accessibility.

However, consideration of various critical factors, like potential heads, is important when evaluating the suitability of sites for hydropower development. This study's primary goal is to evaluate the Furfuro River's potential for hydropower in the Furfuro basin using GIS and SWAT. To find possible hydropower locations in the Furfuro River, this study used multicriteria decision making and the Analytical Hierarchy Process (AHP). Unlike other studies, this study used the new version release of DEM with a higher resolution of 12.5x12.5 m and a long period rainfall record with a grid square of 10 km x10 km.

The potential head differences in the Furfuro River were evaluated by comparing GIS-derived measurements with observed data collected through on-site GPS readings and field measurements. This accuracy assessment aimed to assess the accuracy and reliability of the GIS data in representing real-world conditions and to determine its suitability for hydrological assessments in the study area. This study adopted a minimum spacing of 1,000 meters between consecutive sites to provide sufficient distance for the river ecosystem to recover between hydropower installations. Additionally, only fourth- and fifth-order streams were considered suitable for hydropower production to ensure sufficient flow of water.

2. Materials and Methods

2.1. Study Area

Furfuro River is a perennial river located in the Wulbareg district, Silte zone administration of central Ethiopia. The coordinates of the river are located between Latitude $7^{\circ}40'0''$ to $7^{\circ}54'45''$ N and Longitude $37^{\circ}58'50''$ to $38^{\circ}18'38''$ E (Figure

1). It flows from the high Silte Plateau, descends, and finally merges with the Diyo River before entering Lake Shala. The Furfuro Watershed spans around 202.04 km^2 and has a rough, uneven surface with elevations ranging from 1862 m above sea level to 2669 m above sea level (a.m.s.l.), in the basin of the Rift Valley.

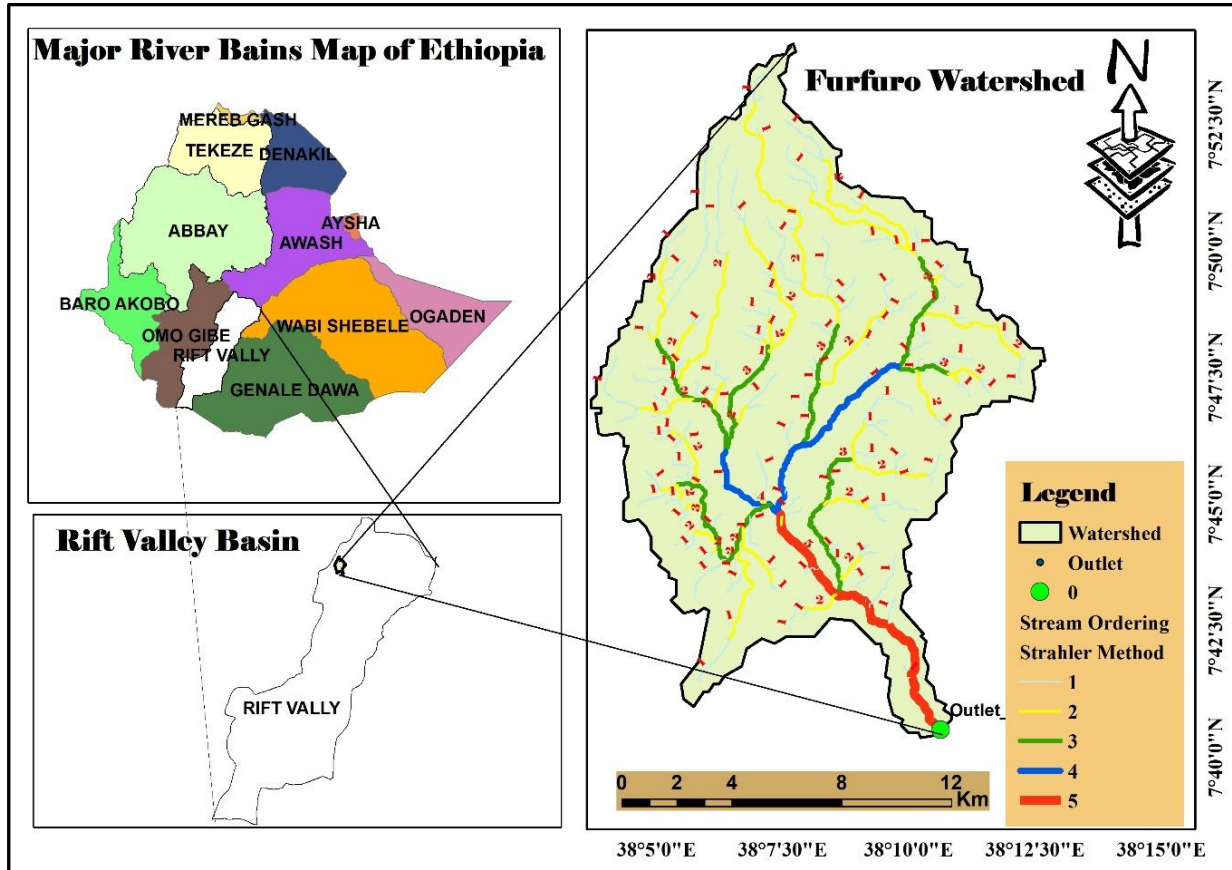


Figure 1. *Furfuro Watershed location map*

2.1.1. DEM

The SWAT model requires the digital elevation model (DEM), which is a crucial part. The large resolution grid DEM of $12.5 \text{ m} \times 12.5 \text{ m}$ was used for the study. The Furfuro basin was split up into smaller watersheds using the DEM. From the DEM, the following parameters were computed: slope, stream order, stream link, and flow accumulation. First, the DEM was used to create the watershed's boundaries. Following project setup and selection of the automated mapping of watersheds, this was completed.

There are five basic processes in the process of delineating a watershed: setting up the DEM, defining the stream, defining the outlet, choosing the watershed outflow, and calculating the sub-basin characteristics. The model determines the flow direction automatically when the DEM setup is finished. Afterwards, stream networks were created, and stream outlets were identified. Finally, the number of subbasins was determined. In the Furfuro watershed, 31 subbasins were delineated (Figure 2), with an estimated total area of 202.04 km^2 .

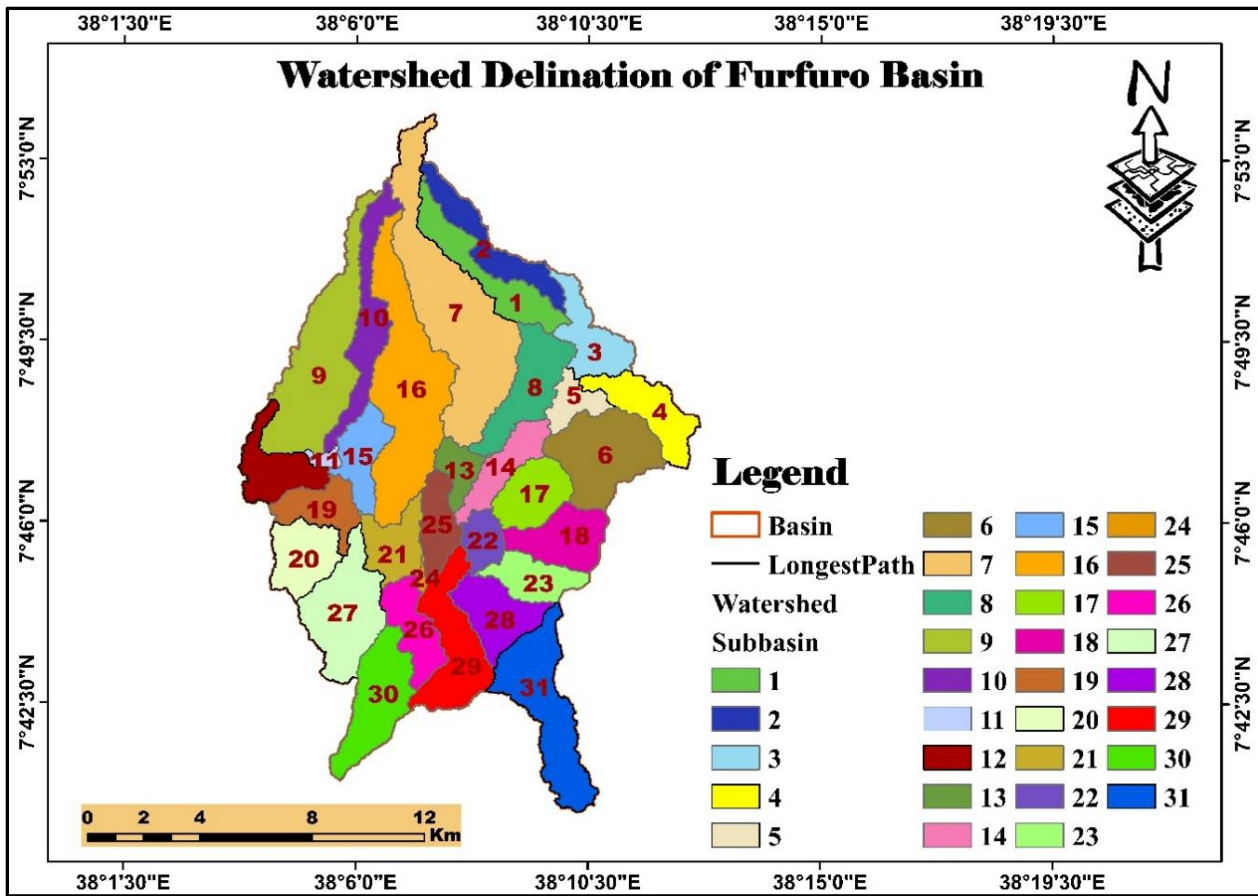


Figure 2. Furfuro watershed delineation.

2.1.2. Soil

The soil database provides data on the upper subsurface and surface of a watershed, which can be used to analyse the types and compositions of soil. The digitized soil database utilized in this study was provided by the MoWE with input from the Food and Agriculture Organization (FAO). In the Furfuro basin, there were two

major soil groups. Furtric Nitosols and plinthic Ferralsols are the two most common soil types in the watershed, as shown in Table 1, with clay being the most common soil type overall. The soil code was created by importing data from the MWSWAT 2012 user soil. MWSWAT, an add-on for MapWindow 4.8.8, provided access to the FAO soil data, which are depicted in Figure 3.

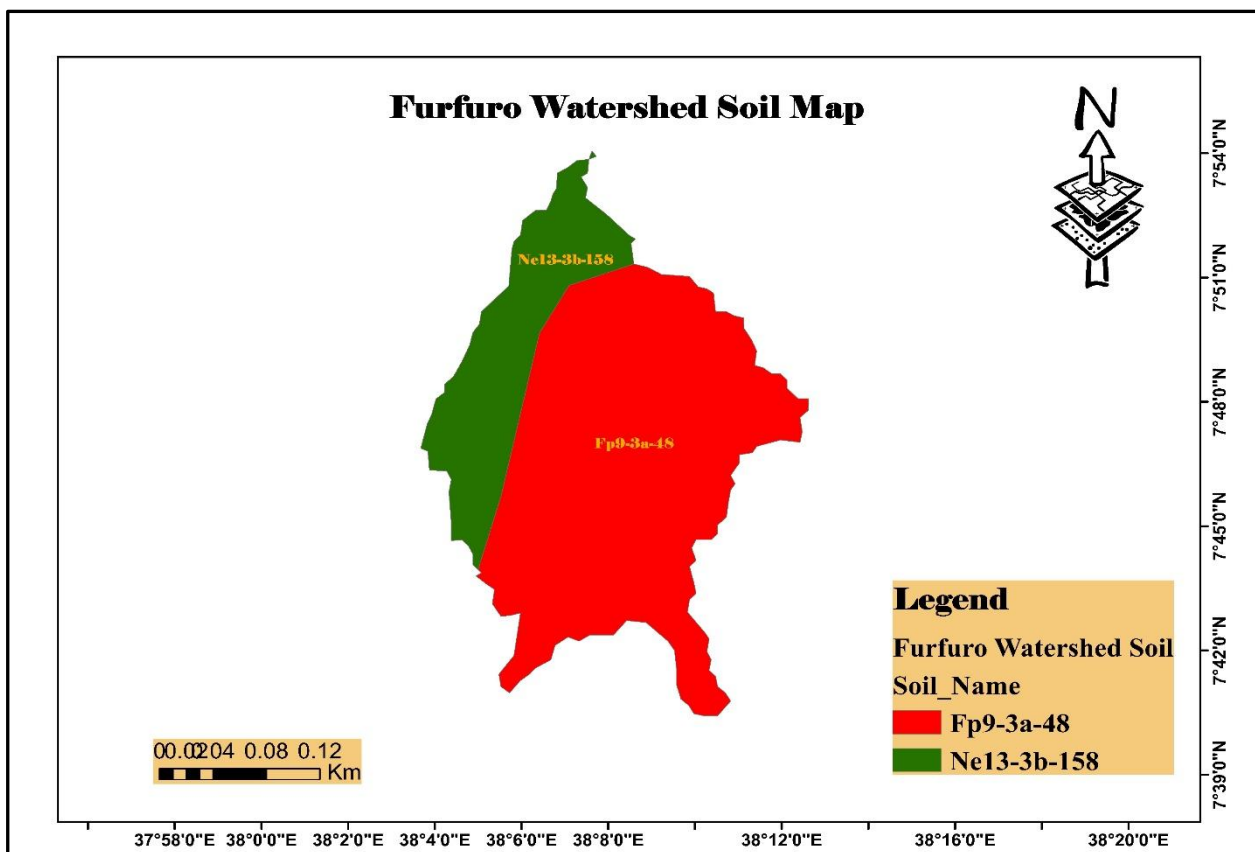


Figure 3. Soil map of Furfuro Watershed

Table 1. Percentage of the covered area for soil data

Soil	Area coverage (km ²)	Percent of area coverage
ferralic nittosols	153.85	77
PPlinthic nittosols.	48.19	23

2.1.3. LULC

The hydrologic response unit of a watershed, which includes runoff, evapotranspiration, and surface erosion, is influenced by land use data. Furfuro Watershed is characterized by various landforms where different soil types are formed, and various vegetation types and tree species grow. Four different land-use classifications

were identified in the research area. In particular, trees (FRST) make up 4% of the basin's total area, range land (RNGE) makes up 25%, the built-up area (URBN) comprises 16%, and within the basin, agricultural land (AGRL) is the most common class of land use, occupying 54% of the basin, followed by rangeland (Figure 4).

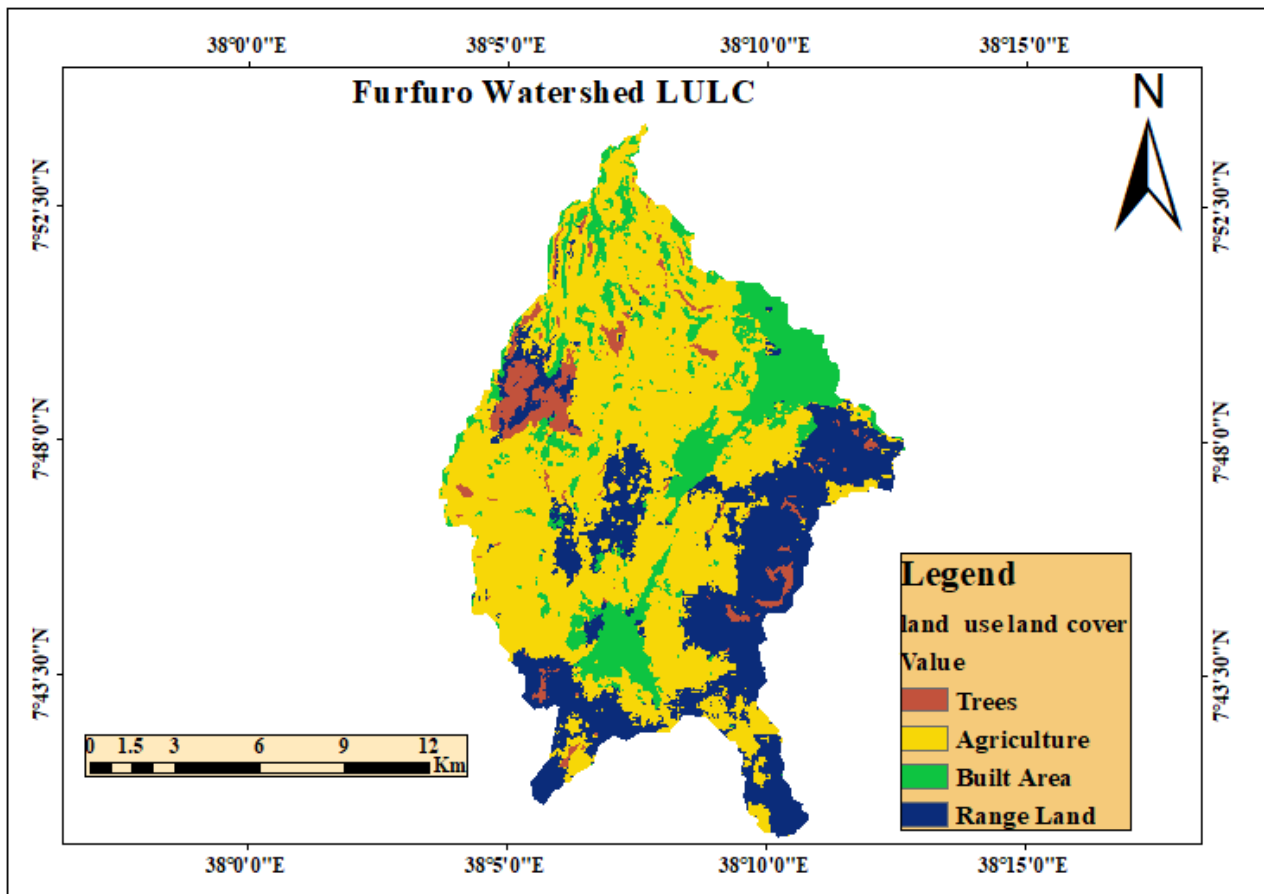


Figure 4. *Furfuro Watershed's LULC*

2.1.4. Climate

Meteorological records are needed to model the catchment's rainfall runoff pattern. Therefore, five metrological stations, both inside and

outside the study area, were strategically selected based on their relative distance from the watershed and data availability, as presented in Figure 5.

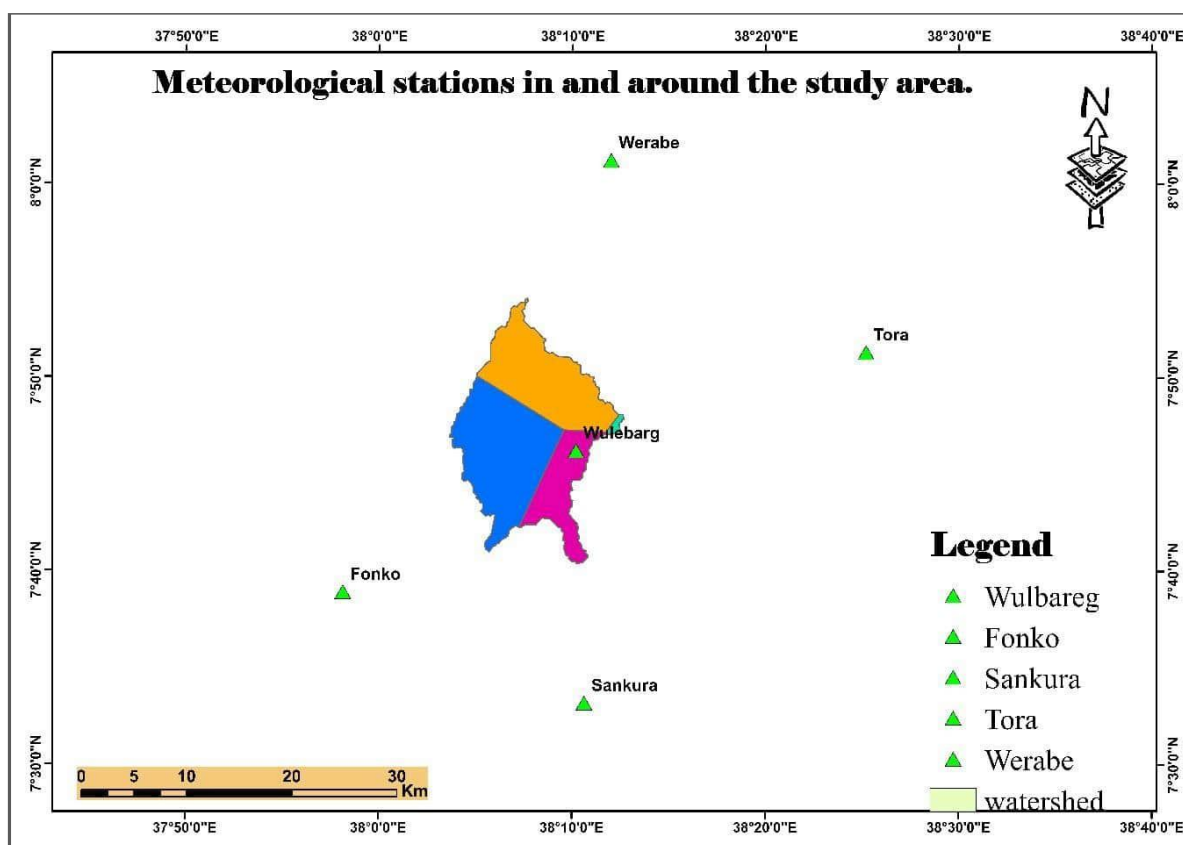


Figure 5. The effect of weather stations inside the study area

The meteorological dataset, which includes daily rainfall, solar radiation, wind speed, relative humidity, and the highest and lowest temperatures for the selected five stations, was obtained from the National Meteorological

Agency at a grid resolution of approximately (5 km × 5 km). Daily data sets spanning a 31-year-long period (1990– 2020) were gathered as shown in Table 2.

Table 2. Weather stations inside and surrounding the research location

No	Station's	Lat	Long	Rain Fall	Min Temp	Max Temp	Solar Radiation	Relative Humidity	Wind speed	Station Class
1	Fonko	7.4	37.6	✓	✗	✗	✗	✗	✗	4
2	Sankura	7.58	37.5	✓	✓	✓	✗	✗	✗	3
3	Tora	7.52	38.3	✓	✗	✗	✗	✗	✗	4
4	Werabe	7.45	38.3	✓	✓	✓	✓	✓	✓	1
5	Wulbareg	7.77	38.2	✓	✓	✓	✗	✗	✗	3

A. Precipitation

The Furfuro River watershed experiences two distinct rainy seasons, characterized by bimodal rainfall patterns. May to October are regarded as the main rainy season, while November through

April is considered the low rainfall season. The watershed has five meteorological stations: Wulbareg is the only station inside the catchment, while the other four are in the surrounding stations, including Tora, Werabe,

Sankura, and Fonko. The watersheds have variations in mean monthly rainfall of 7.02 mm

to 16.67 mm and mean yearly rainfall of 131.77 mm to 194.53 mm, as shown in Figure 5.

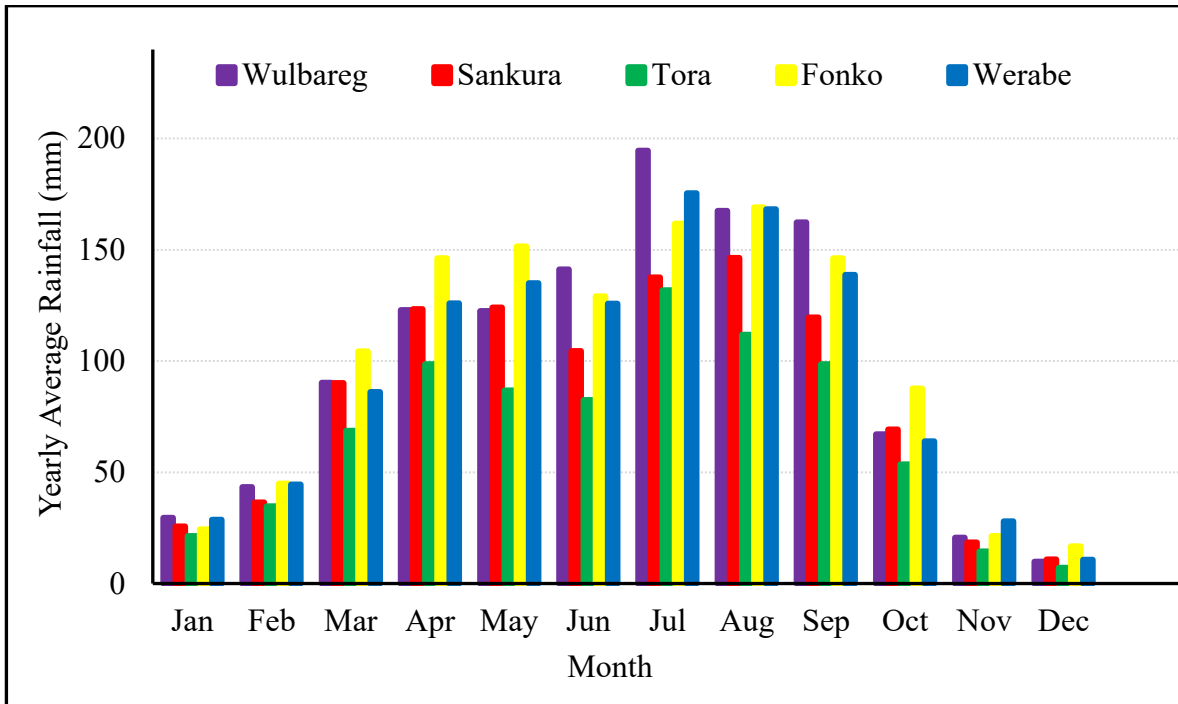


Figure 5. Mean Monthly rainfall at five meteorological stations

B. Temperature

The average monthly minimum temperature in the watershed is between 8.59°C and 13.88°C, while the average monthly maximum temperature is between 21°C and 25.86°C, as

shown in Figure 6. The Furfuro River catchment's meteorological stations' monthly maximum and minimum temperatures were averaged to determine the mean monthly temperature.

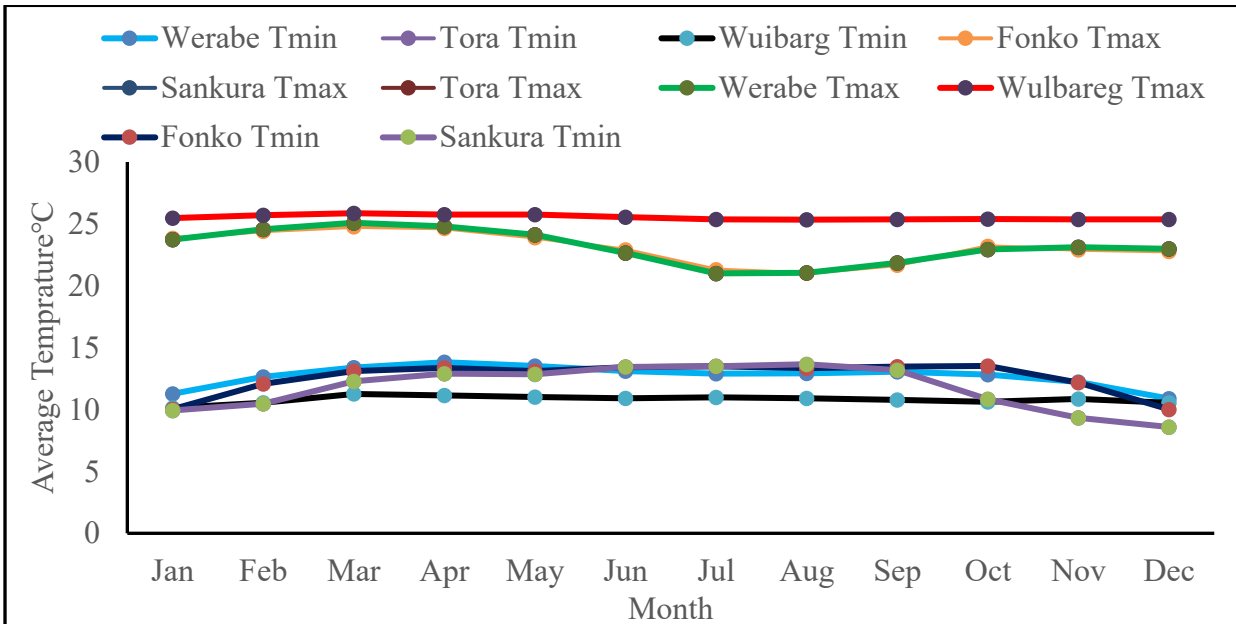


Figure 6. The average monthly high and low temperatures at Walberg station

2.1.5. Filling in Missing Rainfall Data

The data from several stations were missing for a variety of reasons, including the lack of an observer, equipment malfunction, and station relocation. The most popular techniques, such as the arithmetic mean method, the normal ratio method, and the inverse distance approach, were to be applied in order to approximate the missing records (Lebay, 2020).

A. Arithmetic Mean Method

The missing data was calculated by using the arithmetic average of the values from the closest weather station if the average annual precipitation at nearby stations is within 10% of the station with missing data (Sattari & Joudi, 2017).

$$P_x = \frac{1}{n} \sum_{i=1}^n P_i \quad (1)$$

Where: P_i is the precipitation at the first station, P_x is the absent precipitation, and n is the number of adjacent stations.

B. Normal Ratio Method

This technique is applied when the average yearly precipitation of any nearby gauges surpasses 10% of the gauge in question. This evaluates the impact of every nearby station (Adilah & Hannani, 2021).

$$P_x = \frac{1}{n} \sum_{i=1}^n \left(\frac{N_x}{N_i} \right) P_i \quad (2)$$

Where: N_x is the typical annual precipitation for station x , N_i is the typical annual precipitation value for the i th station, and P_x is the precipitation for the same period for the same storm at the interpolation station x .

C. Inverse Distance Method

The most popular and widely accepted technique for identifying missing rainfall data for any scientific investigation is the inverse distance weighting method. With this approach, each sample's weight is inversely related to how far away it is from the predicted point (De Silva et al., 2007).

$$P_x = \frac{\sum_{i=1}^n W_i P_i}{\sum_{i=1}^n W_i} \quad (3)$$

Where: $W_i = \frac{1}{D^2}$, $D^2 = (\Delta X^2 + \Delta Y^2)$ is the station distance in x and y coordinates, taking into account the missing precipitation station at $(0,0)$ position.

P_x = the ungauged station's estimated rainfall

2.1.6. Consistency Test

When evaluating the consistency of a time series data record, like stream flow or rainfall, the double mass curve is a frequently used technique. While the other data set is dubious, the base station is one of the reliable ones. In a diagrammatic manner, the double mass curve procedure compares the two data sets' cumulative values (Weather, 1937). The cumulative rainfall values for each station were plotted, and this allowed us to analyze the consistent characteristics of the rainfall at each station. Additionally, shown in Figure 7 is the outcome of the double mass curve analysis. According to the analysis, all five stations' precipitation data display a linear connection, indicating consistency within the uncertain data set and no deviation from linearity.

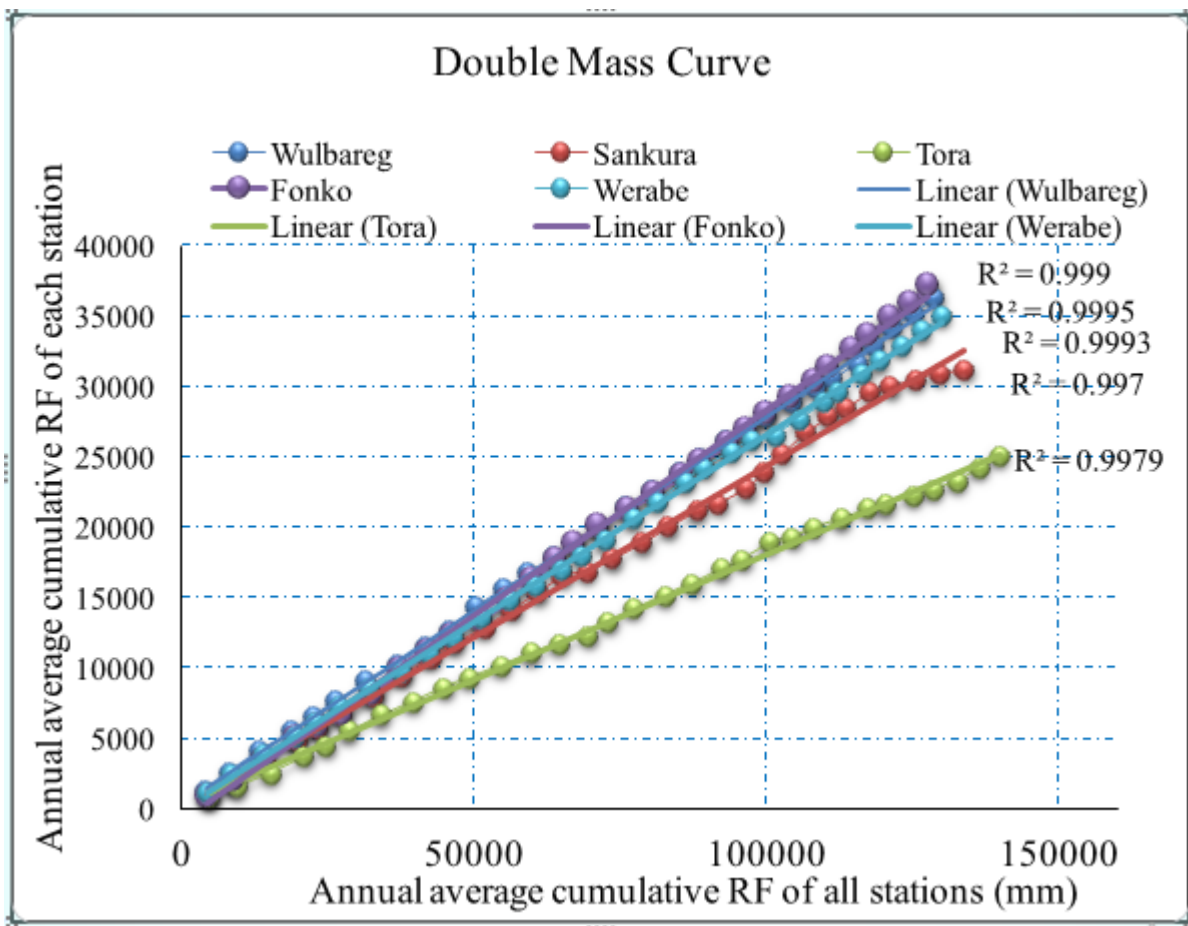


Figure 7. Double mass curve of all stations

2.2. Streamflow data

Streamflow data for the Furfuro River are measured at the Furfuro gauging station (Table 3).

(longitude 38°07'0" and latitude 7°44'0"N), which is located at the watershed's outlet (

Table 3. Furfuro River gauge location and the station's catchment area (data source: MoWE)

Station Name	Latitude	Longitude	Catchment Area Under Station	Recorded Period
Ferfuro	7°44'0"	38°07'0"	153km ²	1992-2007

2.3. Criteria for Selecting Hydropower Potential Sites

To choose a location and identify possible hydropower sites, the following criteria were established (Kusre et al., 2010).

A. Order of Stream:

The Furfuro River network's reaches with sufficient flow for power generation were identified using stream ordering. Stream order is

a technique for stream sorting that splits a network of streams into reaches and displays the flow rate over those reaches. The Strahler approach was selected above the other stream ordering techniques, including the Shreve, Horton, and Strahler methods, because of its broad applicability and ease of use (Strahler, 1958).

When two streams of the same order meet, this method results in a higher stream order; for example, two first-order streams that border one another create a second-order stream, and more. Therefore, a larger flow magnitude is typically the outcome of better stream order (Arthur et al., 2020). Only streams in the 5th and 4th orders of magnitude are taken into consideration when choosing locations to guarantee an adequate flow of water for the production of hydropower.

DEM was processed in ArcGIS using the fill tool to remove any depressions. Next, Calculations were made for flow direction and flow accumulations. Flow accumulation was created with a threshold of 4,000 cells using ArcMap's raster calculator. The results from the raster calculator were then used to organize and create the stream network of the Furfuro River using the stream order tool, as shown in Figure 8.

B. Head Drop

Potential head is a critical parameter for assessing a hydropower potential site and can be

measured through direct measurement, topographic maps, and Google Earth Pro (Genet et al., 2024) and (Pandey et al., 2015). In this study, the 3D Analyst tool in ArcGIS was utilized to extract the longitudinal profile from DEM data, considering a minimum distance of 1000 meters between two consecutive sites to allow the river environment to recuperate between hydropower stations. Overlying the DEM of the watershed and the river network that was formed during the watershed delineation, the potential head drop at each specific sub-basin was estimated as shown in Figure 9.

C. Stream Order

The hydrology tool on the raster calculator was used to create the stream network for the Furfuro River. Cells exceeding a threshold of 4,000 were classified into 1 stream of 5th order, 2 streams of 4th order, and 5 streams of 3rd order, as shown in Figure 8.

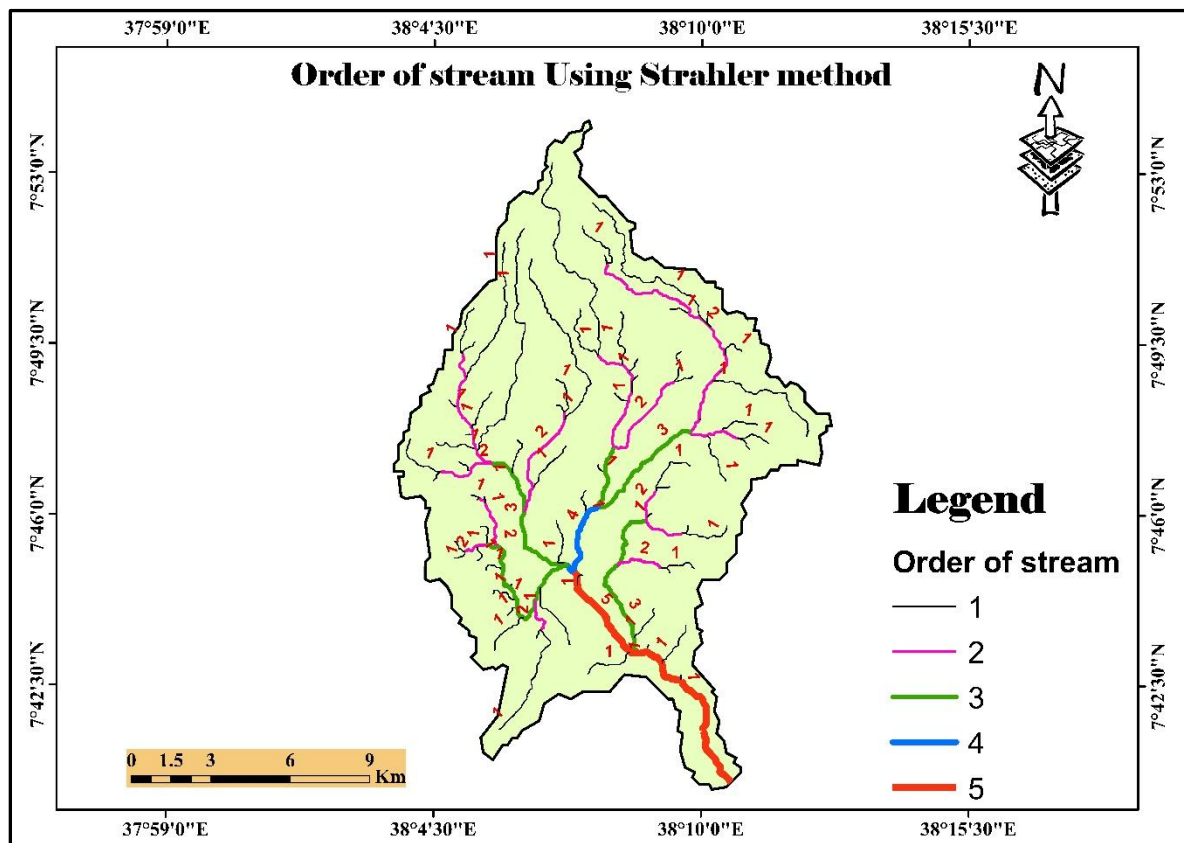


Figure 8. Stream order by the Strahler method

2.4. Selection of Hydrological Model

Hydrologic models are reduced to conceptual depictions of a certain hydrologic cycle stage. The hydrologic estimation and prediction were their main application. When choosing hydrologic models, there are several critical elements to consider, including Data availability, study objectives, required accuracy, program cost, acquisition costs, computer processing speed, and user support (Bajracharya, 2015). The model with the lowest parameters and least variety is the one that performs the best, producing results that are almost perfect duplicates of reality. There are three categories for hydrological models: distributed, semi-distributed, and lumped models. In lumped hydrologic models, the hydrological parameters are regarded as uniform across the area and are determined at that level. Despite the low requirement for data, the lumped model may not be as useful in integrated management due to its inability to adequately represent the regional heterogeneity of the environment (Devia et al., 2015).

Several smaller sub-basins make up the basin in semi-distributed models, sharing the same characteristics but allowing the hydrologic parameters to vary to some extent at the sub-basin level. In terms of the way it represents geographic variability and the amount of data needed; semi-distributed model is a middle ground between distributed and lumped models. Compared to fully distributed models, these models need less input data and have a greater physical basis than lumped models (Bajracharya, 2015). In distributed hydrological models, a given basin is divided into smaller cells, allowing for complete parameter variation. As a result, the basin is shown more accurately, and the hydrological processes are well explained. However, there are a lot of limitations due to data requirements and processing capacity.

Models often use concepts from mathematics and statistics to relate certain inputs (like temperature, rainfall, etc.) to the model output (like runoff). With the use of GIS and hydrological models (SWAT), it is now possible to integrate all physical occurrences, improving physical world simulation (Kusre et al., 2010). For this study, the SWAT model was chosen because it can simulate multiple hydrological components, perform large-scale simulations, and facilitate long-term impact studies with readily available information. It is freely available, compatible with ArcGIS, and supported by a vibrant and supportive user community.

2.5. Analysis of Hydrological Response Units

The consistent soil, land use, and management factors are represented by the hydrologic response units (HRUs). The HRU entities were defined by choosing 10 % identification for the soil, slope, and land use/cover, and the runoff for each HRU unit was simulated by overlaying the classified land use/land cover, soil, and slope data. Thereafter, the simulated HRU runoff was used to estimate the overall runoff generation for each sub-basin in the watershed. Using mean monthly streamflow data from the Ferfuro Gauging Station between 1992 and 2007, the sensitivity of streamflow parameters in a SWAT model was assessed. SUFI-2, which is used for the calibration, uncertainty, and sensitivity analysis of hydrological models, uses the SWAT-CUP (SWAT Calibration and Uncertainty Programs) framework to efficiently identify the key variables that influence the model's outputs. The sensitivity rank was determined using the t-sat and P-values, and the model performance to replicate the observed stream flow data was assessed using the NSE, R^2 , and PBIAS metric indexes.

2.6. Weather Generator

Climate data is one of the primary inputs that SWAT uses to mimic the hydrological processes. The model must incorporate all daily values of the climatic variables from measured data or generated from an accessible station. Ethiopia, like the majority of poor nations, lacks accurate and thorough long-term climatic data. Consequently, by producing data from the existing climate stations, the weather generator resolves this issue. To store and interpret daily weather data for use with SWAT projects, the SWAT Weather Database was created as a user-friendly application. It can quickly create text (.txt) files and save relevant daily weather information (Guide, 2016). Depending on the availability of climatic data and its representativeness to the study area's climatic condition, only Werabe Station was selected as the synoptic station used for generating the remaining weather data for other weather

generator stations. Among the five stations used in this study (Wulbareg, Tora, Fonko, Sakura, and Werabe), only the Werabe station has a continuous climatic data record, so the Werabe station is used for calculating the WGEN statistic.

2.7. Data collection and analysis

The primary requirement to conduct the research was data collection. The research required collecting spatial and temporal data from various sources. Two main data collection methods, primary and secondary, were used to gather the necessary data and information. Secondary data collection techniques were used to get most of the data for this research; however, certain data, such as elevation along the river using hand GPS and watershed outlet data, were obtained through primary data collection methods.

Table 4. *Type of data, source, and availability of data*

No	Data Types	Sources	Purpose
1	DEM	AlasKa. S.F	12.5*12.5 m resolution to analyze the spatial information.
2	Land use/land cover raster map	Esri Portal (Global Land Cover)	10*10 m resolution map of 2022.
3	Soil Data	Food and Agriculture Organization of the United Nations (FAO)	250*250m (tentative) resolution map, soil layer attributes for each soil layer.
4	Daily weather data	National Meteorological Service Agency (NMSA)	Daily precipitation, maximum and lowest temperatures, wind speed, relative humidity, and solar radiation.
5	Daily stream flow data	Ministry of Water and Energy (MoWE)	Daily streamflow from the Furfuro station for calibration and validation

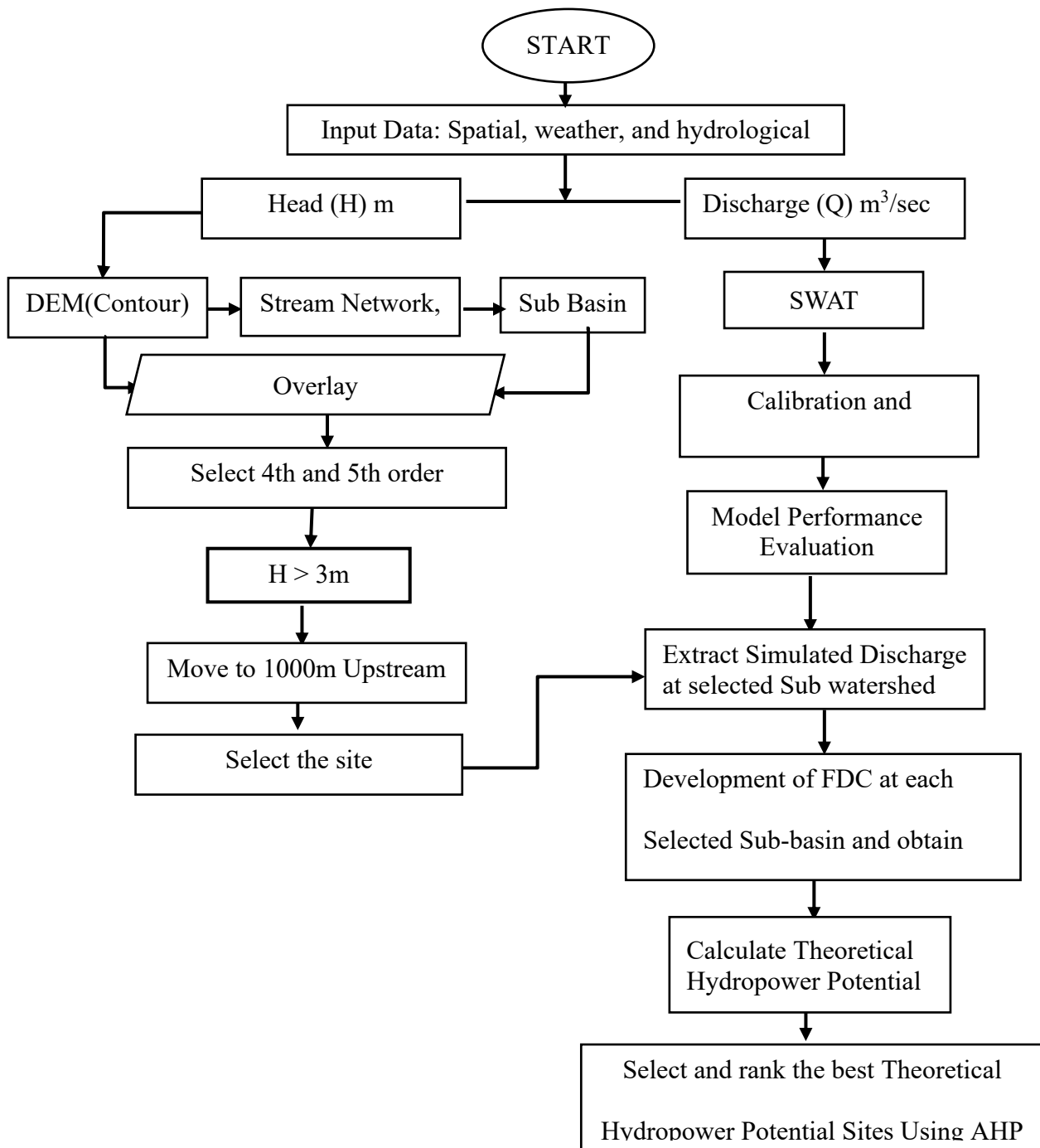


Figure 9. Procedure for assessing theoretical hydropower potential (Bhattarai et al., 2024)

2.8. Hydropower Site Selection Using Multi-Criteria Decision Making Methods

Weighted Linear Combination (WLC), the Technique for Order Preference by Similarity to Ideal Solution (TOPSIS), fuzzy-based methods, and the Analytic Hierarchy Process (AHP) are some of the MCDM techniques that are processed using GIS. While TOPSIS works well for resolving energy-related issues, AHP is

strongly advised for assessing assessment criteria and alternative solutions. (Dimitra G. Vagiona, 2021).

2.8.1. Analytical Hierarchy Process (AHP) Method

One of the most popular multi-criteria decision-making techniques is the Analytic Hierarchy Process (AHP) method, which is employed when both objective and subjective considerations

must be taken into account. It is useful for planning conventional and renewable energy sources, allocating energy resources, managing building energy, and planning electric utilities. The AHP procedure can be divided into three parts: identifying a hierarchy of objectives, criteria, and alternatives; performing pairwise comparisons between criteria; and calculating the relative importance of each element at all level Table 5.

According to Saaty (1980), to achieve consistent comparisons between criteria, he proposed a scale with nine absolute numbers representing the intensity of relative importance between two criteria. erical value 1 on this scale represents equal importance, while a value of 9 indicates factors that are extremely important in relation to other aspects, as shown in

Table 5. Saaty's Scale of Intensity and Relative Importance, Source (Saaty, 1980)

Intensity of Importance	Definition
1	Equal importance
3	moderate importance of one over another
5	Essential or strong importance
7	Very strong importance
9	Extreme importance
2,4,6,8	Intermediate values between the two adjacent judgments

3. Results and Discussion

The results and discussion contain the following major parts: head determination, hydrological modeling results, estimation of theoretical power potential for selected sites, and prioritization and ranking of the best suitable hydropower sites.

3.1. Head Drop Determination

3.1.1. Head Determination for Sub-Basin 31

In order to evaluate a study area's hydropower potential, one important variable is potential locations, estimated in **Error! Reference source not found.**

head. Based on the sub-basin's topographic characteristics, this head is determined. The 3D Analyst tool in ArcGIS was utilized to extract the longitudinal profile from DEM data in order to compute the head drop. The river network that was formed during the watershed delineation for selected sub-basins chosen to estimate the flow out was specified for this process. The head drop is determined from the extracted longitudinal profile as the variation in elevation along the stream course between its highest and lowest

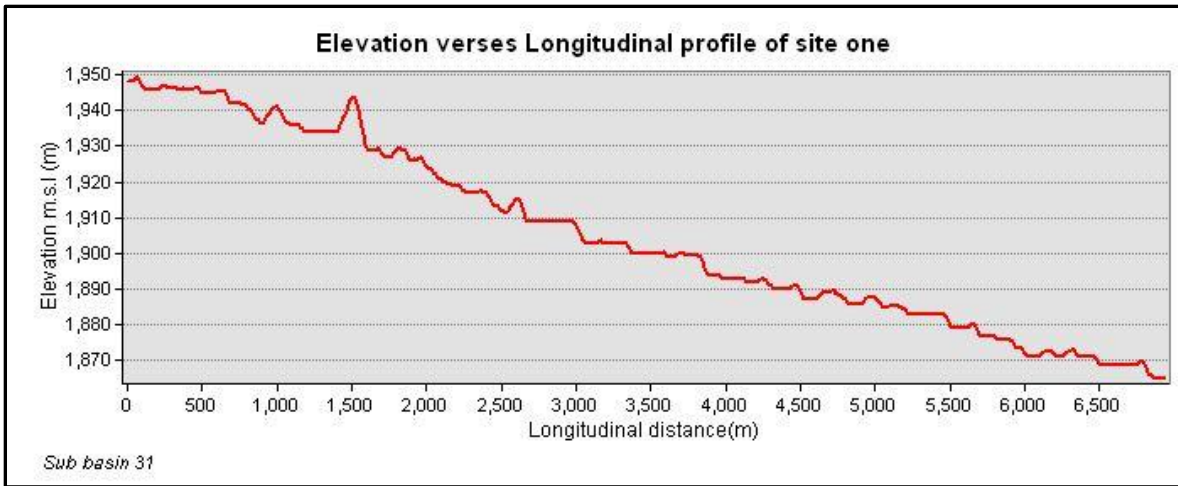


Figure 10. Elevation profile for sub-basin 31

Elevation profile for sub-basin 31 (**Error! Reference source not found.**) shows a longitudinal distance of 6000 meters. The head drop, which is the variation between the

highest elevation point (1949 meters) and the lowest elevation point (1864meters), is 85meters.

3.1.2. Head Determination for Sub-Basin 29

The same procedure was followed at Site One above to determine the head difference of Site 2, -sub-basin 29.

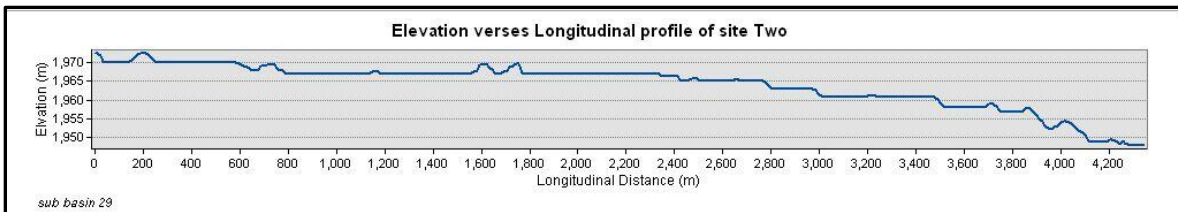


Figure 11. Elevation profile for sub-basin 29

Elevation profile for sub-basin 29 (Figure 11) shows a longitudinal distance of 4310 meters. The head drop, which is the variation between the highest elevation point (1990 meters) and the lowest elevation point (1945 meters), is 45 meters.

3.1.3. Head Determination for Sub-Basin 24

The same procedure was followed at Site above to determine the head difference of Site 3 -sub-basin 24.

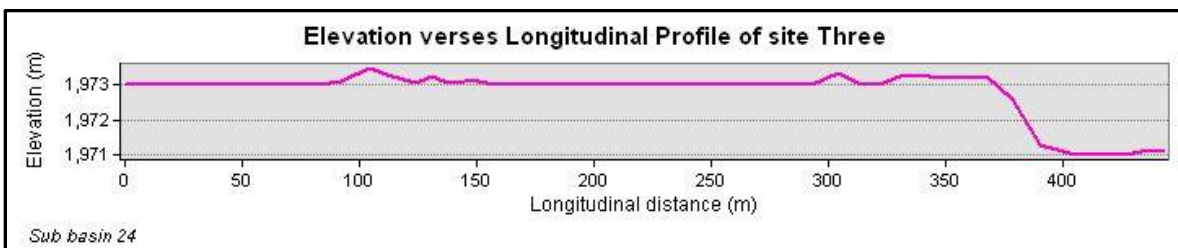


Figure 12. Elevation profile for sub-basin 24

Elevation profile for sub-basin 24 (Figure 12) shows a longitudinal distance of 420 meters. The head drop, which is the variation between the highest elevation point (1974 meters) and the lowest elevation point (1971 meters), is 3 meters.

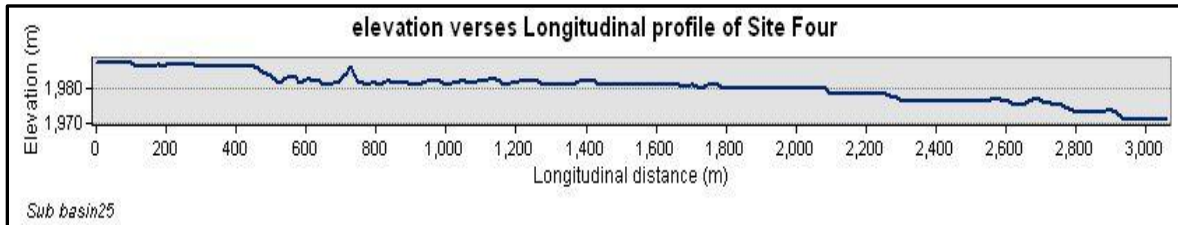


Figure 13. Elevation profile for sub-basin 25

Elevation profile for sub-basin 25 (Figure 13) shows a longitudinal distance of 3020 meters. The head drop, which is the variation between the highest elevation point (1989 meters) and the lowest elevation point (1971 meters), is 18 meters.

3.1.4. Head Determination for Sub-Basin 25

The same procedure was followed at Site above to determine the head difference of Site 4 -sub-basin 25.

3.2. Result of the Hydrological Model

3.2.1. Sensitivity Analysis

265 HRUs were accounted for in the analysis. Every HRU has a different mix of soil type and land usage. The most vulnerable model

parameters for the Furfuro watershed were identified using a global sensitivity analysis using the SWAT CUP algorithms. Twelve of the 24 factors were found to be the most sensitive after multiple iterations of the sensitivity analysis, as provided in

Table 6. According to (Abbaspour, 2015b), a larger absolute value of the t-stat and, as shown in (Figure 14), a smaller p-value ($p < 0.5$) indicate greater sensitivity of a parameter.

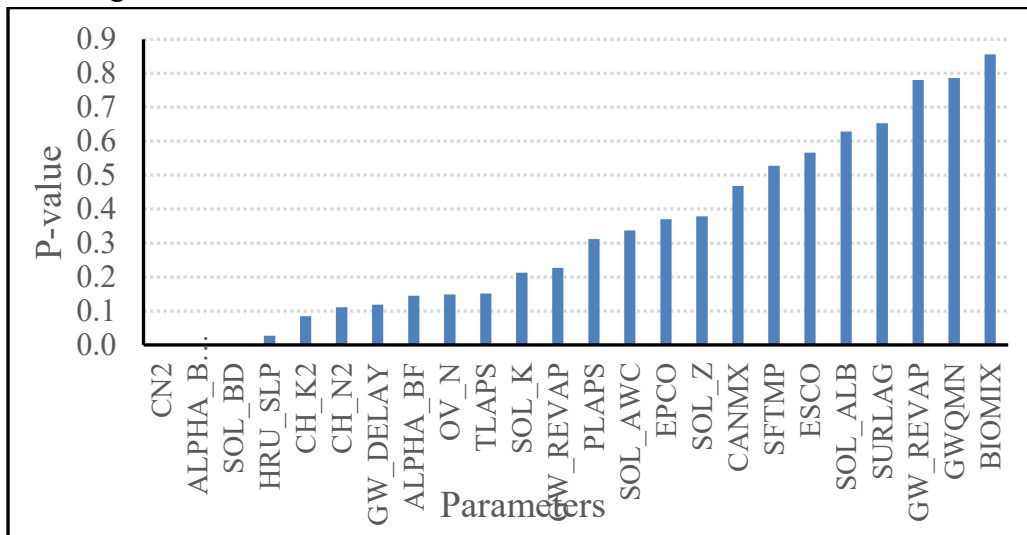


Figure 14. Sensitive parameters and their p-value

Table 6. *The Furfuro watershed's sensitive flow parameters are ranked*

Parameter Name	t -stat	p-value	Sensitivity rank
CN2	12.76	0	1
ALPHA_BNK	10.72	0	2
SOL_BD	10.56	0	3
HRU_SLP	2.21	0.03	4
CH_K2	-1.73	0.08	5
CH_N2	-1.59	0.11	6
GW_DELAY	-1.56	0.12	7
ALPHA_BF	-1.46	0.15	8
OV_N	1.45	0.15	9
TLAPS	1.44	0.15	10
SOL_K	-1.25	0.21	11
GW_REVAP	1.21	0.23	12

3.2.2. Calibration

Parameters that were found to have higher sensitivity were adjusted to calibrate the model. Twelve of the identified high-sensitivity parameters were chosen for calibration in this Table 7. For comparison, the table also includes the recommended SWAT limits for the indicated

study. Calibration was carried out repeatedly until the discrepancy between the actual and predicted values was as small as possible. The calibrated parameters are shown together with their numerical values in parameters. The calibrated parameter values are within the recommended ranges.

Table 7. *Summary of Calibrated Flow Parameters*

No	Parameter Name	Fitted Value	Min_value	Max_value
1	CN2	-0.19	-0.2	0.2
2	ALPHA_BF	0.12	0	1
3	GW_DELAY	168.09	30	450
4	GW_REVAP	0.19	-0.02	0.2
5	CH_N2	0.23	0	0.3
6	CH_K2	24.02	0.01	500
7	ALPHA_BNK	0.03	0	1
8	SOL_K	1154.4	0	2000
9	SOL_BD	1.61	0.9	2.5
10	HRU_SLP	0.76	0	1
11	OV_N	15.17	0.01	30
12	TLAPS	-4.41	-10	10

The adjusted parameter values were compared with the findings of other researchers, demonstrating a dependence on the characteristics of the watershed. (Anore et al., 2025) Adjusted 9 parameters in a study conducted on the MMegech watershed on the Omo Gebie basin of Ethiopia. While (Bhattarai et al., 2024) obtained a reasonable degree of agreement between the simulated and observed outcomes in the Sunkoshi river basin in Nepal by adjusting 12 parameters. Similarly, (Kusre et al., 2010) in the Kopili River basin in Assam, India, adjusted 7 parameters, and (Pandey et al., 2015)

in the Mat River, southern Mizoram, India, adjusted 6 parameters.

In this study, it can be concluded that the parameters selected for calibration were good candidates to characterize the physical parameters of the furfuro watershed. The model was calibrated for 7 years of data, from 1994 to 2000. The performance index of the model calibration was calculated as a coefficient of determination (R^2) value of 0.69, an NSE value of 0.68, and a PBIAS value of -3.5. The monthly streamflow calibration data show that there is high agreement between the simulated and observed streams, according to.

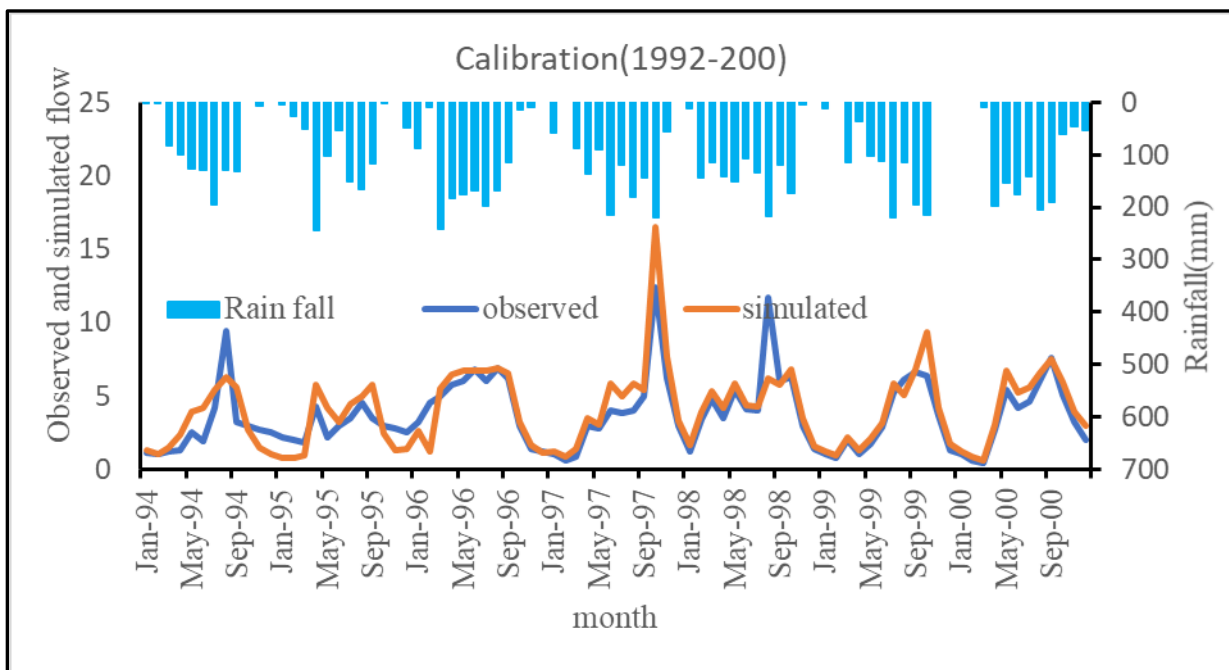


Figure 15. Calibration result of the SWAT-CUP for the period 1994–2000

As shown in Figure 15, the SWAT-CUP calibration results for the years 1994–2000. In 1994 and 1998, the peak values were somewhat underestimated, but the model well represents the overall flow trend. Additionally, a 95PPU plot showing the values of the simulated and actual monthly stream flow data shows a satisfactory linear connection.

3.2.3. Validation

After calibrating the model, the calibrated parameters were used for validation. Data on observed streamflow collected between 2001 and 2007 at the Furfuro River outlet were used to validate the model. Input parameters used in the calibration step were the same ones used to run the model during the validation (Abbaspour, 2015a). The simulated flows for seven periods between 2001 and 2007 were validated once

calibration was completed, and acceptable values of R^2 , NSE, and PBIAS were obtained. Monthly flows were used to check the validation. The results of the current study were compared with those of prior studies. This study showed a good agreement with (Moshe & Tegegne, 2022). Assessed the run-of-river hydropower potential in the data-scarce region, Omo-Gibe Basin, Ethiopia. In this study, the potential head was directly measured from the GIS digital feature class, which could bring a higher variation in the

actual observed head. (Anore et al., 2025) Used GIS Multi-criteria decision-making to identify potential hydropower generation sites in Megecha watershed, Omo Gebie Basin of Ethiopia, and (Pandey et al., 2015) showed good agreement. Additionally, the generated and actual monthly flow agreed well, according to the model validation, according to (Moriasi et al., 2007), with a coefficient of determination (R^2) value of 0.65, an NSE value of 0.64, and a PBIAS value of -1.8.

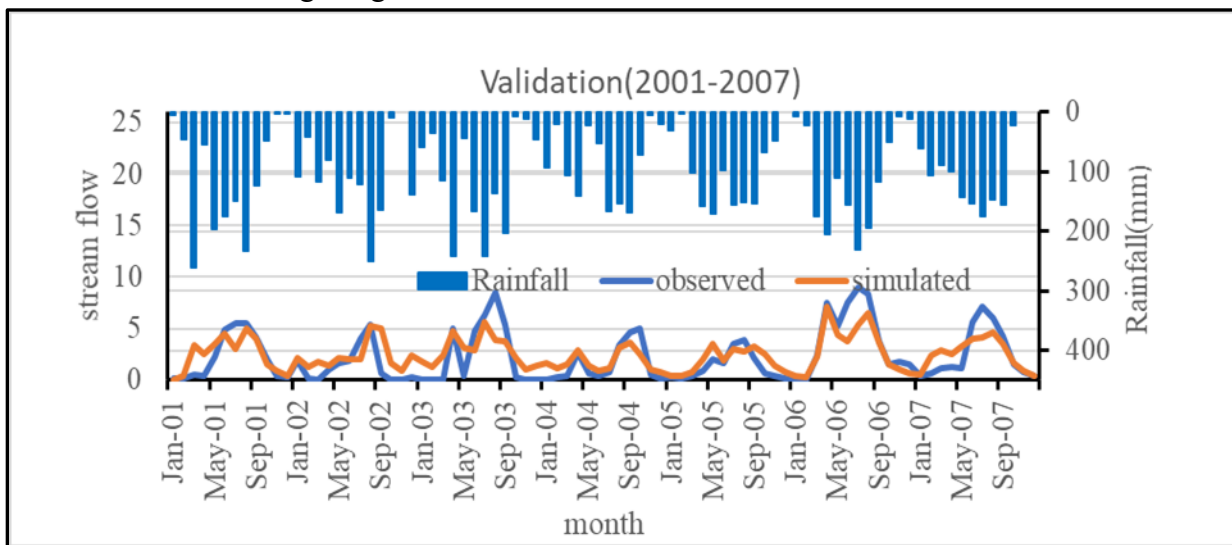


Figure 16. Validation result of the SWAT-CUP for the period of 2001–2007

As shown in Figure 16, the SWAT-CUP validation results for the years 2001–2007 indicate that peak values were slightly underestimated during 2003, 2006, and 2007. Therefore, the validated model of the Furfuro watershed can be used to predict the spatial and temporal availability for the evaluation of hydropower potential.

3.2.4. Flow Duration Curve (FDC)

For the purpose of evaluating hydropower potential, flow duration curves show the river's

temporal flow characteristics. The percentage of time that the streamflow is expected to reach or exceed a critical value for hydropower production. The Furfuro Watershed has been divided into 31 sub-watersheds of the thirty-one sub-basins, taking into account the confluence of two streams of the second order and above as outflow sites. Four of these sub-watersheds were chosen to assess their hydropower potential because they contain fourth and fifth-order streams with a head of three meters or more, as shown in Figure 17.

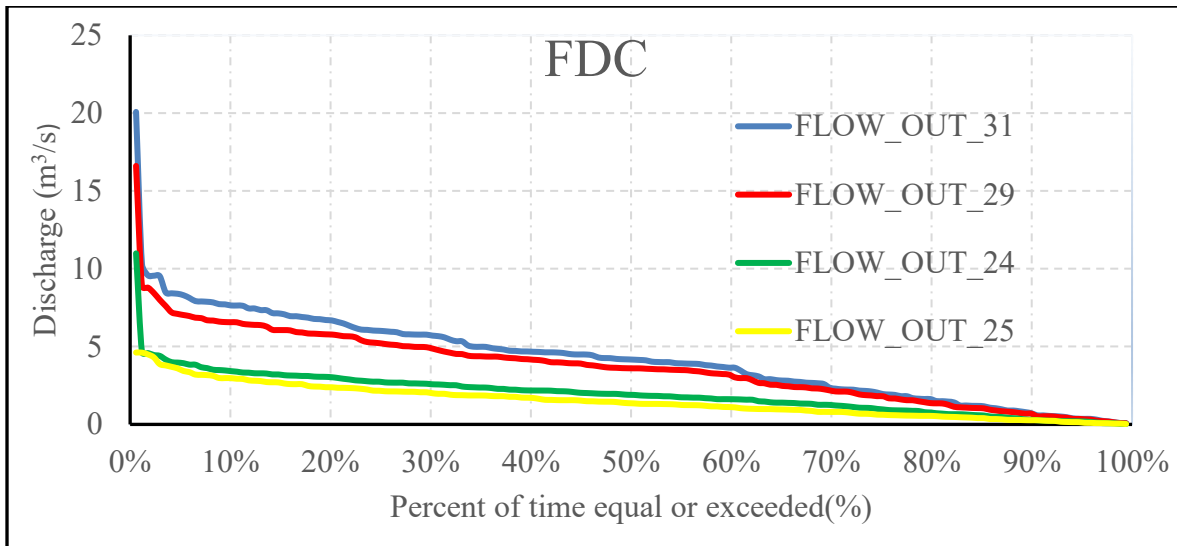


Figure 17. Flow duration curve for the Furfuro River at different HP sites

The flow duration curve from 1994–2007 (168 months) indicates that the highest flow ranges from 20.08 to 4.62 m³/s and occurs 0%–10% of the time. The curve in this region has a relatively steep slope, indicating that flood events occur with high intensity and short-duration rain. The flow duration curve shows that for a moderate slope with a flow of 6.68 m³/s to 1.94 m³/s, the percentage of the year is 20%. For 90% to 95% of the year, the flow typically ranges between 0.36 m³/s and 0.1 m³/s. The important exceedance percentages of Q30, Q40, Q50, Q60, Q70, Q80, Q90, and Q95 are taken into consideration for depicting the flow characteristics of the chosen sites in order to summarize the final results of the flow duration curves for the four sites. Finally, at site 1, the

discharge at Q30 is 5.71 m³/s, and the firm flow (dependable) is 0.36 m³/s at Q95.

3.3. Theoretical Hydropower Potential Estimation

The theoretical hydropower potential considers gross head drop without considering any losses and the river's timely flow. For the four sites that were chosen, this study created power duration curves to illustrate how each location's hydropower potential changed over time. The identified locations' theoretical hydropower was evaluated using standard power equations after the streams' head and FDC characterization. Selected stream segments' theoretical power potential at key exceedance percentages for all hydropower plants (Figure 18).

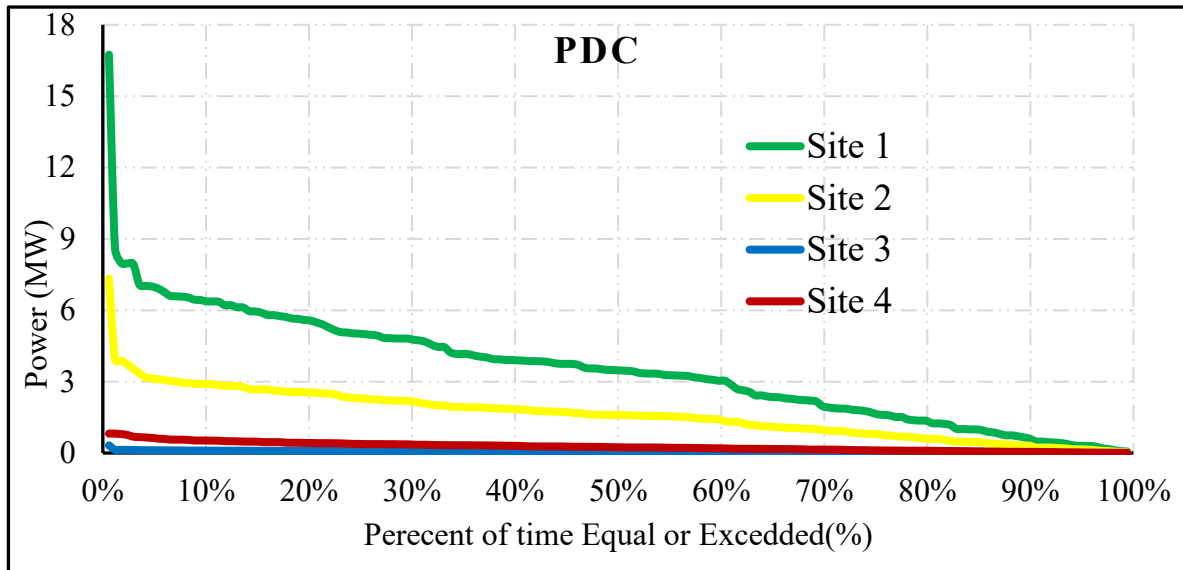


Figure 18. Power duration curve for selected HP sites at the Furfuro River

As shown in Figure 18, the maximum theoretical power (P30) at Q30 is 4757.95 KW, 2150.74 KW, 75.84 KW, and 353.69 KW. Site 1 (sub-basin 31) has the maximum firm power generation (P95) of all the identified sites, with a capacity of 297.77 KW, and Site 4 (sub-basin 25)

has the minimum firm power generation capacity of 18.36 KW. The result in Table 4.6 indicates the total theoretical power generation of all sites identified in the catchment with 30%, 40%, 50%, 60%, 70%, 80%, 90%, and 95% flow exceedances.

Table 8. Theoretical Hydropower at Key Exceedance Percentages of Selected Sub-basins

% (time)	Site 1	Site 2	Site 3	Site 4
	FLOW_OUT_31 (m ³ /s)	FLOW_OUT_29 (m ³ /s)	FLOW_OUT_24 (m ³ /s)	FLOW_OUT_25 (m ³ /s)
Q30	5.71	4.87	2.58	2.00
Q40	4.67	4.16	2.18	1.70
Q50	4.16	3.60	1.90	1.35
Q60	3.64	3.20	1.62	1.12
Q70	2.36	2.19	1.25	0.80
Q80	1.50	1.35	0.72	0.53
Q90	0.72	0.69	0.30	0.27
Q95	0.36	0.32	0.19	0.10

According to the selected sites, 1, 2, and 4 are all classified under Micro hydropower potential sites (11–500 KW), and site 3 is classified under a Pico hydropower site (<10 KW). Ethiopia

classifies its hydropower systems differently from other countries. For the categorization of hydropower, there is no widely recognized standard.

3.4. AHP-Based Hydropower Potential Site Prioritization

The rating of the sites is crucial to assist local decision-makers in making a logical judgment regarding which sites to prioritize for the chosen sites. A comprehensive review of the critical

factors that affect prioritization of potential sites has been made, as presented in Table 9. Due to data limitations, only power, discharge, head, accessibility, and site distance were taken into account in this study, even though many criteria affected the ranking of the sites.

Table 9. *The criteria used in earlier investigations in comparison to this study's findings*

No	Previous studies	To determine the possible locations, factors were employed	Prioritized sites
1	(Anore et al., 2025)	Road accessibility and demand center from every location	To identify suitable potential sites for Hydropower
2	(Vinchurkar & Samtani, 2019)	Head, discharge, total efficiency, number of turbines, cost per unit of power, field observations, and professional judgment	The total rank weights were used to determine the possible location.
3	(Teshome, n.d.)	In-stream power, Discharge, Head, and accessibility to roads	Prioritization of a suitable hydropower potential site

3.4.1. Pair-wise Comparison of Criteria

This approach helps in determining when two factors are equally important or if one is more crucial for a particular issue. Simplify a difficult

issue and make it easier to choose appropriate weights for many factors. Each pairwise comparison matrix element is assigned based on the intensity of the importance scale.

Table 10. *Pairwise Comparison Matrix*

Criteria	Power	Discharge	Head	Accessibility	Distance
Power	1	2	2	4	5
Discharge	1/2	1	2	5	4
Head	1/2	1/2	1	4	5
Accessibility	1/4	1/5	¼	1	3
Distance	1/5	1/4	1/5	1/3	1
Sum	2.45	3.95	5.45	14.3	18

3.4.2. Critical Weight Calculation

Following matrix normalization, the crucial weights were determined by averaging the

corresponding values in each column, as indicated in Table 11.

Table 11. Critical Weight Calculation

Criteria	Power	Discharge	Head	Accessibility	Distance	Criteria Weight
Power	0.41	0.51	0.37	0.28	0.28	0.37
Discharge	0.20	0.25	0.37	0.35	0.22	0.28
Head	0.20	0.13	0.18	0.28	0.28	0.21
Accessibility	0.10	0.05	0.05	0.07	0.17	0.09
Distance	0.08	0.06	0.04	0.02	0.06	0.05

3.4.3. Calculating Consistency Ratio

According to Saaty's (1980) Analytic Hierarchy Process (AHP), the consistency of a pairwise comparison matrix is assessed using a numerical measure known as the consistency ratio (CR). The consistency index (CI) to average consistency index (RI) ratio is shown by this indicator. Finding the largest Eigenvalue, or λ_{max} , is necessary before calculating the consistency index value. This can be done by **Table 12**, and a corresponding value of RI for $n = 5$ is 1.12, as shown in Table 13.

multiplying the pairwise comparison matrix by the criteria weight values from the normalization matrix. The weighted sum value is then calculated by adding the values in the rows. The ratio of each weighted sum value to the corresponding criteria weight is then determined, and the average ratio of the weighted sum value to the criteria weight is λ_{max} . This calculation yields a λ_{max} value of 5.29, as shown in .

Table 12. λ_{max} Calculation

Weighted Sum Value	Criteria Weight	Ratio: WSV/CW	λ_{max}
1.96	0.37	5.34	26.43/5=5.29
1.53	0.28	5.50	
1.15	0.21	5.35	
0.44	0.09	5.11	
0.27	0.05	5.13	
Sum		26.43	

$$CI = \frac{\lambda_{max} - n}{n - 1} = \frac{5.29 - 5}{5 - 1} = 0.07 \quad (4)$$

Table 13. Random Consistency Index (Saaty, 1980)

N	1	2	3	4	5	6	7	8	9	10
RI	0	0	0.6	0.9	1.12	1.24	1.3	1.41	1.45	1.49

$$CR = \frac{CI}{RI} = \frac{0.07}{1.12} = 0.06 < 0.01 (\text{acceptable}) \quad (5)$$

As a result, the 0.06 CR value is below the permitted CR value. Therefore, it is acceptable that the pairwise comparison is consistent.

Consequently, power received a higher weight (37%) than discharge (28%) among the five criteria for priority analysis. The head, weighing twenty-one percent, is the third factor. Road proximity or accessibility ranks fourth with a

percentage of 9%. The final factor is distance, which has a 5% weight.

The best site among the options was selected using a combination of these five parameters.

The Score code to constrain the factor could be maximized or minimized and was formulated for each prospective hydropower site as shown in Table 14.

Table 14. Standardize the criterion code for the selection of the most suitable site among prospective sites

Criteria	Objective
Power	Maximize
Discharge	Maximize
Head	Maximize
Accessibility	Maximize
Distance	Minimize

The suitability index for each prospective hydropower site was calculated

using the criterion formulated as shown in Table 15.

Table 15. Ratings for Selected Sites Based on Standardized Criteria

Site	P95(KW)	Q95(m ³ /s)	Head(m)	Accessibility	Distance b/n Site and Town (Km)
1	1	1	1.00	0.50	2.31
2	0.48	0.91	0.42	1.00	1.00
3	0.02	0.52	0.07	0.50	1.21
4	0.06	0.29	0.15	0.50	3.95

3.5. Ranking the Furfuro Watershed's Hydropower Sites

A pair-wise comparison matrix produced by the Analytic Hierarchy Process (AHP) serves as the foundation for the ranking procedure. The weighted index is established by using weighted linear combination analysis. Each appropriateness score is standardized as part of this process, and weight indexes are assigned to represent the proportional value of each score. The weight indexes and standardized suitability are then added up to determine the overall site appropriateness score. This score efficiently

assesses each hydropower site's suitability. The appropriateness index for each hydropower site in the study region is calculated using the formula below.

$$SI = (P * 0.37)(Q * 0.28) + (H * 0.21) + (A * 0.09) + (D * 0.05) \quad (6)$$

The sites are then prioritized for hydropower development based on their appropriateness index, which was calculated from this analysis. The top ranking goes to the site with the highest appropriateness index value shown in Table 16.

Table 16. *Hydropower Sites' Final Suitability Ranks in the Furfuro Watershed*

Site	P95(KW)	Q95(m ³ /s)	Head(m)	Accessibility	Distance b/n Site and Town (Km)	Suitability Index (SI)	Rank
1	297.77	0.36	85	1.00	3.03	0.89	1
2	143.38	0.32	45	2.00	1.31	0.60	2
3	5.50	0.19	3	1	1.59	0.21	3
4	18.36	0.10	18	1.00	5.18	0.18	4

With a theoretical hydropower capacity of 0.297 MW and a discharge rate of 0.36 m³/s at 95% exceedance in the Furfuro River, Site 1 is considered the most suitable site due to its greatest suitability index (0.89). On the other

hand, with a theoretical hydropower capacity of 0.018 MW and a discharge of 0.1 m³/s at 95% exceedance, Site 4 is the least suited location. All the selected potential hydropower sites are located on the mainstream of the Furfuro River, as shown in Figure 19.

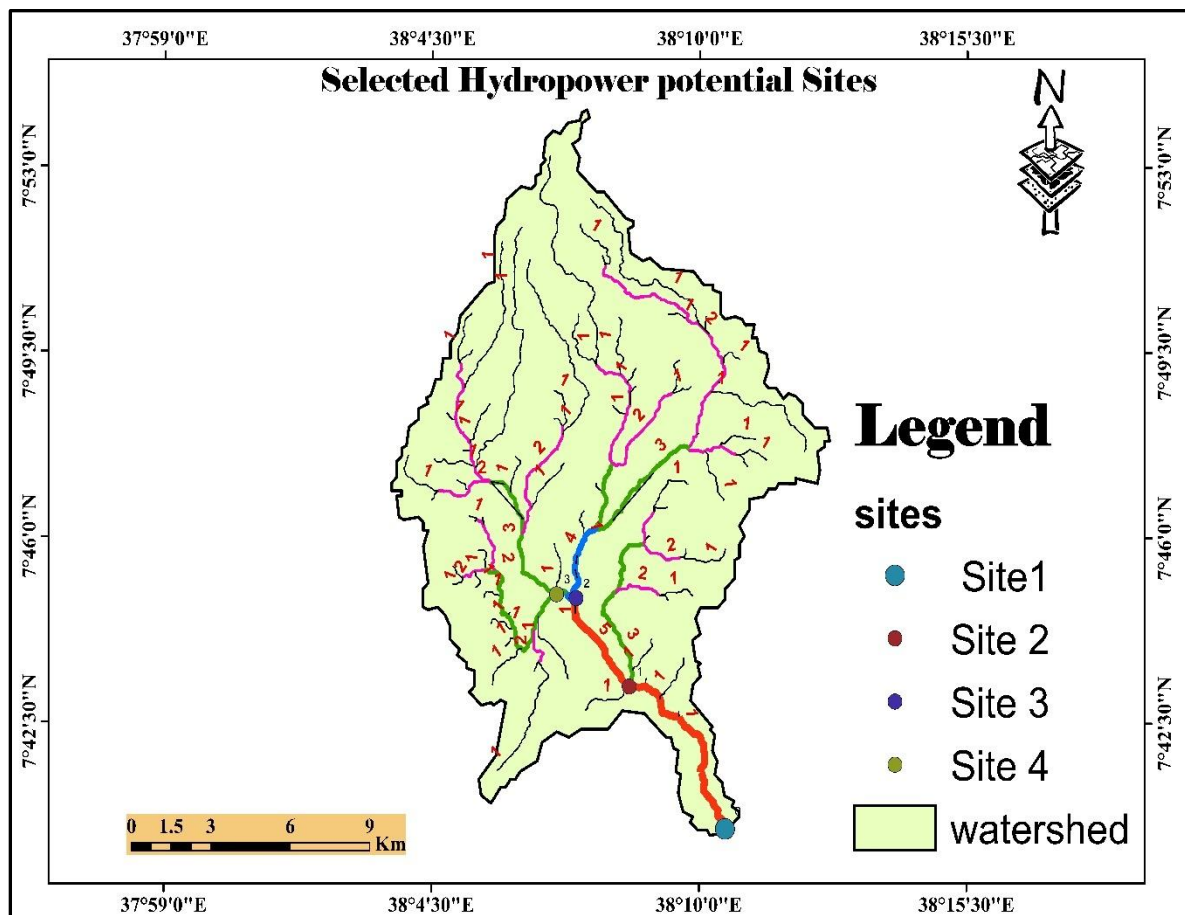


Figure 19. *Map of the selected hydropower potential sites*

4. Conclusions

This study used GIS and SWAT hydrological modeling to assess the hydropower potential of

the Furfuro River. Among the 31 potential sites, only four were selected based on higher-order streams. The potential candidate sites showed a

range of gross head values between 3 and 85 meters. With a theoretical hydropower capacity of 0.297 MW and a discharge rate of 0.36 m³/s at 95% exceedance in the Furfuro River, Site 1 is determined to be the optimum site through a multi-criteria decision analysis utilizing the AHP technique. On the other hand, with a theoretical hydropower capacity of 0.018 MW and a discharge of 0.1 m³/s at 95% exceedance, Site 4 is the least suited location. This investigation highlights the effectiveness of integrating GIS, SWAT modeling, and multi-criteria decision analysis for identifying optimal hydropower sites while considering crucial factors such as head, power discharge, accessibility, and the distance to the closest town.

The power produced can be utilized by the communities residing in the catchment. People in the study area lack access to energy, and there is a lack of sustainable and readily available energy sources. These communities currently rely on traditional sources of energy. Micro hydropower plants, on the other hand, can enhance rural communities' standard of living while assessing

in environmental preservation. Future studies should assess the effects of climate change on the Furfuro River's streamflow regime and include economic analysis. Only a theoretical assessment of hydropower potential is included in the present study.

Authorship contribution:

Writing original draft, A.G.E, Data collection and model parameterization, A.E.M, conceptualization, Editing, Reviewing, T.Z.A, reviewing, A.T.B, Data collection, T.K.H, methodology and validation, M.T.T.

Data Availability: Data can be acquired upon request.

Conflicts of Interest: The authors declare that they have no conflicts of interest.

Acknowledgments: The authors would like to thank the Ministry of Water and Energy and the Ethiopian National Meteorological Service Agency for providing the required data.

References

- Abbaspour, K. C. (2015a). SWAT calibration and uncertainty programs (CUP). Neprashtechology.Ca. <https://doi.org/10.1007/s00402-009-1032-4>
- Abbaspour, K. C. (2015b). SWAT calibration techniques: Calibration/validation periods, calibration/validation procedures, hydrology - first and foremost.
- Anore, H. W., Lohani, T. K., & Ayalew, A. T. (2025). Identification of potential hydropower generation sites using geospatial techniques in the Megecha watershed of Ethiopia. *Heliyon*, 11(2), e42063. <https://doi.org/10.1016/j.heliyon.2025.e42063>
- Arthur, E., Anyemedu, F. O. K., Gyamfi, C., Asantewaa Tannor, P., Adjei, K. A., Anornu, G. K., & Odai, S. N. (2020). Potential for small hydropower development in the Lower Pra River Basin, Ghana. *Journal of Hydrology: Regional Studies*, 32, 100757. <https://doi.org/10.1016/j.ejrh.2020.100757>
- Bajracharya, I. (2015). Assessment of run-of-river hydropower potential and power supply planning in Nepal using hydro resources [Unpublished master's thesis]. Institut Für Energietechnik Und Thermodynamik.
- Bhattarai, R., Mishra, B. K., Bhattarai, D., Khatiwada, D., Kumar, P., & Meraj, G. (2024). Assessing hydropower potential in Nepal's Sunkoshi River Basin: An integrated GIS and SWAT

- hydrological modeling approach. *Scientifica*, 2024, Article 1007081. <https://doi.org/10.1155/2024/1007081>
- De Silva, R. P., Dayawansa, N. D. K., & Ratnasiri, M. D. (2007). A comparison of methods used in estimating missing rainfall data. *Journal of Agricultural Sciences*, 3(2), 101–108. <https://doi.org/10.4038/jas.v3i2.8107>
- Devia, G. K., Ganasri, B. P., & Dwarakish, G. S. (2015). A review on hydrological models. *Aquatic Procedia*, 4, 1001–1007. <https://doi.org/10.1016/j.aqpro.2015.02.126>
- Dimitra G. Vagiona. (2021). Comparative multicriteria analysis methods for ranking sites for solar farm deployment: A case study in Greece. *International Journal of the Analytic Hierarchy Process*, 13(2). <https://doi.org/10.13033/ijahp.v13i2.833>
- Ebhota, W. S., & Tabakov, P. Y. (2019). Power supply and the role hydropower plays in Sub-Saharan Africa's modern energy system and socioeconomic wellbeing. *International Journal of Low-Carbon Technologies*, 14*(3), 347–363. <https://doi.org/10.1093/ijlct/ctz031>
- Ejargew, A., Genet, A., & Tegenu, M. T. (2025). Assessment of hydropower potential for rural electrification: A case study of the Waleme River. *American Journal of Energy Engineering*, 13(5), 101–108.
- Eshetu, S. (2024). Fuelwood from natural forests' contribution to households' energy use and its effect on carbon dioxide emission in Delanta District, Northeastern Ethiopia. *Energy, Ecology and Environment*, 9(3), 245-260.
- Genet, A., Tadesse, A., Zelalem, T., & Kifle, T. (2024). Assessment of head for hydropower potential using DEM, Google Earth, and GPS in the Furfuro Watershed, Ethiopia. *International Journal of Engineering Research & Technology*, 8(2), 80–88.
- Guide, A. Q. (2016). Weather database.
- Klunne, W. J. (2013). Small hydropower in Southern Africa: An overview of five countries in the region. *Journal of Energy in Southern Africa*, 24(3), 14–25. <https://doi.org/10.17159/2413-3051/2013/v24i3a3138>
- Kusre, B. C., Baruah, D. C., Bordoloi, P. K., & Patra, S. C. (2010). Assessment of hydropower potential using GIS and hydrological modeling technique in Kopili River basin in Assam (India). *Applied Energy*, 87(1), 298–309. <https://doi.org/10.1016/j.apenergy.2009.07.019>
- Lebay, M. (2020). Techniques of filling missing values of daily and monthly rainfall data: A review. *SF Journal of Environmental and Earth Science*, 3(1), 1020.
- Meder, K., & Bubbenzer, P. O. (2011). Application of environment assessment related to GIZ ECO micro hydropower plants in the Sidama Zone/Ethiopia [Diplomarbeit, Universität].
- Moriasi, D. N., Arnold, J. G., Van Liew, M. W., Bingner, R. L., Harmel, R. D., & Veith, T. L. (2007). Model evaluation guidelines for systematic quantification of accuracy in watershed simulations. *Transactions of the ASABE*, 50(3), 885–900. <https://doi.org/10.13031/2013.23153>
- Mose, N., & Kipchirchir, E. (2024). Foreign direct investment and economic growth in Kenya: A comprehensive analysis. *Asian Journal of Economics, Business and Accounting*, 24(2), 1–13. <https://doi.org/10.9734/AJEBA/2024/v24i21215>
- Moshe, A., & Tegegne, G. (2022). Assessment of run-of-river hydropower potential in the data-scarce region, Omo-Gibe Basin, Ethiopia. *International Journal of Energy and Water Resources*, 6(4), 531–542. <https://doi.org/10.1007/s42108-022-00192-2>

- Nadiatul Adilah, A. A. G., & Hannani, H. (2021). Comparison of methods to estimate missing rainfall data for short term period at UMP Gambang. *IOP Conference Series: Earth and Environmental Science*, 682(1), 012027. <https://doi.org/10.1088/1755-1315/682/1/012027>
- Pandey, A., Lalrempuia, D., & Jain, S. K. (2015). Assessment of hydropower potential using spatial technology and SWAT modelling in the Mat River, southern Mizoram, India. *Hydrological Sciences Journal*, 60(10), 1651–1665. <https://doi.org/10.1080/02626667.2014.943669>
- Saaty, T. L. (1980). *The analytic hierarchy process: Planning, priority setting, resource allocation*. McGraw-Hill.
- Sattari, M. T., & Joudi, A. R. (2017). A comparative analysis of artificial neural networks and neuro-fuzzy models for missing precipitation data estimation. *Hydrology Research*, 48(6), 1735–1751. <https://doi.org/10.2166/nh.2016.364>
- Sharmin, F., & Khan, M. R. (2016). A causal relationship between energy consumption, energy prices and economic growth in Africa. *International Journal of Energy Economics and Policy*, 6(3), 477–494.
- Strahler, A. N. (1958). Dimensional analysis applied to fluvially eroded landforms. *Geological Society of America Bulletin*, 69(3), 279–300. [https://doi.org/10.1130/0016-7606\(1958\)69](https://doi.org/10.1130/0016-7606(1958)69)
- Surendra, K. C., Takara, D., Hashimoto, A. G., & Khanal, S. K. (2014). Biogas as a sustainable energy source for developing countries: Opportunities and challenges. *Renewable and Sustainable Energy Reviews*, 31, 846–859. <https://doi.org/10.1016/j.rser.2013.12.015>
- Teshome, A. (n.d.). Assessment of hydropower potential using geospatial technology in a case study of Guna-Tana landscape Upper Abay Basin, Ethiopia.
- Tilahun, A. (2011). Assessment of micro hydro power potential of selected Ethiopian rivers-a case study in the North-West part of the country. *East African Journal of Energy*, 14(5), 670–679.
- Vinchurkar, S. H., & Samtani, B. K. (2019). Performance evaluation of the hydropower plants using various multi-criteria decision-making techniques. *International Journal of Engineering and Advanced Technology*, 8(6), 2131–2138. <https://doi.org/10.35940/ijeat.F8490.088619>
- World Bank. (2011). *World development report 2011: Conflict, security, and development*. The World Bank. <https://doi.org/10.1596/978-0-8213-8439-8>